Physica Scripta. Vol. 61, 675–689, 2000

Large-scale Breit-Pauli R-matrix Calculations for Transition Probabilities of Fe V

Sultana N. Nahar and Anil K. Pradhan

Department of Astronomy, The Ohio State University, Columbus, Ohio 43210, U.S.A.

Received August 6, 1999; accepted in revised form November 12, 1999

Abstract

Ab initio theoretical calculations are reported for the electric (El) dipole allowed and intercombination fine structure transitions in Fe V using the Breit–Pauli R-matrix (BPRM) method. We obtain 3865 bound fine structure levels of Fe V and 1.46×10^6 oscillator strengths, Einstein A-coefficients and line strengths. In addition to the relativistic effects, the intermediate coupling calculations include extensive electron correlation effects that represent the complex configuration interaction (CI). For bound-bound transitions the BPRM method, based on atomic collision theory, entails the computation of the CI wavefunctions of the atomic system as an (electron + target ion) complex. The target ion Fe VI is represented by an eigenfunction expansion of 19 fine structure levels dominated by the spectroscopic configuration $3d^3$, and a number of correlation configurations. Fe V bound levels are obtained with angular and spin symmetries $SL\pi$ and $J\pi$ of the (e + Fe VI) system such that $2S + 1 = 5,3,1$, $L \leq 10$, $J \leq 8$. The bound levels are obtained as solutions of the Breit-Pauli (e + ion) Hamiltonian for each $J\pi$, and are designated according to the 'collision' channel quantum numbers. A major task has been the identification of these large number of bound fine structure levels in terms of standard spectroscopic designations. A new scheme, based on the analysis of quantum defects and channel wavefunctions, has been developed. The identification scheme aims particularly to determine the completeness of the results in terms of all possible bound levels with $n \leq 10, l \leq n-1$, for applications to analysis of experimental measurements and plasma modeling. Sample results are presented and the accuracy of the results is discussed. A comparison of the dipole length and velocity oscillator strengths is presented, indicating an uncertainty of 10–20% for most transitions.

1. Introduction

Transition probabilities of heavy elements, particularly the iron group, are of great importance in astrophysical and laboratory sources. Fuhr *et al.* [1] have compiled data from a number of available sources. However, the accuracy and the extent of these data is largely inadequate for many general applications such as the calculation of local thermodynamic equilibrium (LTE) stellar opacities [2,3], and radiative levitation and accelerations of heavy elements [4]. Among the particular applications including Fe V as a prominent spectral constituent are the the non-LTE models of Fe V spectra in hot stars [5], and the observed extreme ultraviolet Fe V emission from young white dwarfs [6]. For example, currently available data for Fe V fails to account for the observed opacity of iron in the XUV region where observations of newly formed hot and young white dwarfs clearly show Fe V lines [6]. In all of these applications it is highly desirable to have as complete a dataset of radiative transition probabilities as possible. While the twin problems of completeness and accuracy pose a challenge to the theoretical methods, they are of interest not only in various applications but may also be of use in the analysis of experimental measurements of observed energy levels of complex atomic systems from the iron group.

The Opacity Project (OP) [7,2] and the Iron Project (IP) [8] laid the foundation for large-scale theoretical calculations using *ab intio* methods. The R-matrix method [9], based on atomic collision theory techniques and adapted for the OP [10] and the IP [8], has proven to be very efficient for these calculations. Whereas the OP calculations were all in the *LS* coupling approximation, with no relativistic effects included, the subsequent IP work is in intermediate coupling using the Breit-Pauli extension of the R-matrix method [8]. While most of the IP work has concentrated on collisional calculations, recent works have extended the BPRM method to radiative bound-bound and bound-free calculations for transition probabilities [11], photoionization [12], and (electro-ion) recombination [13]. The first comprehensive BPRM calculation of fine structure transition probabilities was carried out for the highly charged ions Fe XXIV and Fe XXV [11] that are of special interest in X-ray astronomy. Very good agreement was found with existing results available for a limited number of transitions but using very accurate theoretical methods including relativistic and QED effects [14,15], thus establishing the achievable accuracy for the BPRM calculations. However those He-like and Li-like atomic systems are relatively simple, and the electron correlation effects relatively weak, compared to the low ionization stages of iron group elements. The present work attempts to enlarge the scope of the possible BPRM calculations to include the iron group elements, as well as to solve some outstanding problems related to level identifications in *ab initio* theoretical calculations using collision theory methods.

Unlike atomic structure calculations, where the electronic configurations are pre-specified and the levels identified, the bound levels calculated by collision theory methods adopted in the OP and the IP need to be identified since only the channel quantum numbers are known for the bound states corresponding to the (e + ion) Hamiltonian of a given total angular and spin symmetry $SL\pi$ or $J\pi$. The precise correspondence between the channels of the collision complex, and the bound levels, must therefore be determined. The problem is non-trivial for complex atoms and ions with many highly mixed levels due to configuration interaction. In the OP work, carried out in *LS* coupling, this problem was solved by an analysis based on quantum defects and the numerical components of wavefunctions in the region outside the R-matrix boundary (that envelops the target ion orbitals). The present work extends that treatment to the analysis of fine structure levels computed in intermediate

coupling. In addition, considerable effort is devoted to the determination of the completeness of the set of computed bound levels; comparison with the expected levels derived from all possible combination of angular and spin quantum numbers reveals the missing levels. The general procedure could be applied to spectroscopic measurements and the analysis of observed levels of a given atomic system by comparison with the theoretical predictions.

2. Theory

The general theory for the calculation of bound states in the close coupling (CC) approximation of atomic collision theory, using the R-matrix method, is described by Burke and Seaton [16] and Seaton [17]. The application to the Opacity Project work is described by Seaton [7], Berrington *et al.* [10], and Seaton *et al.* [2]. The relativistic extensions of the R-matrix method in the Breit–Pauli approximation are discussed by Scott and Taylor [18], and the computational details by Berrington, Eissner, and Norrington [19]. The application to the Iron Project work is outlined in Hummer *et al.* [8].

In the present work we describe the salient features of the theory and computations as they pertain to large-scale BPRM calculations for complex atomic systems. Identification of fine structure energy levels is discussed in detail.

Following standard collision theory nomenclature, we refer to the (e + ion) complex in terms of the 'target' ion, with N bound electrons, and a 'free' electron that may be either bound or continuum. The total energy of the system is either negative or positive; negative eigenvalues of the $(N+1)$-electron Hamiltonian correspond to bound states of the (e + ion) system. In the coupled channel or close coupling (CC) approximation the wavefunction expansion, $\Psi(E)$, for a total spin and angular symmetry $SL\pi$ or $J\pi$, of the $(N+1)$ electron system is represented in terms of the target ion states as:

$$\Psi_E(\mathrm{e+ion}) = A\sum_i \chi_i(\mathrm{ion})\theta_i + \sum_j c_j\Phi_j, \tag{1}$$

where χ_i is the target ion wave function in a specific state $S_iL_i\pi_i$ or level $J_i\pi_i$, and θ_i is the wave function for the $(N+1)$th electron in a channel labeled as $S_iL_i(J_i)\pi_i\ k_i^2\ell_i(SL\pi)\ [J\pi]$; $k_i^2(=\varepsilon_i)$ is the incident kinetic energy. In the second sum the Φ_j's are correlation wavefunctions of the $(N+1)$ electron system that (a) compensate for the orthogonality conditions between the continuum and the bound orbitals, and (b) represent additional short-range correlation that is often of crucial importance in scattering and radiative CC calculations for each $SL\pi$.

The functions $\Psi(E)$ are given by the R-matrix method in an inner region $r \le a$. These are bounded at the origin and contain radial functions that satisfy a logarithmic boundary condition at $r = a$ [20]. In the outer region $r > a$ the inner region functions are matched to a set of linearly independent functions that correspond to all possible (e + ion) channels of a given symmetry $SL\pi$ or $J\pi$. The outer region wavefunctions are computed for all channels, $(C_tS_tL_t\pi_t)\varepsilon l$, where C_t is the target configuration, and used to determine the individual channel contributions (called "channel weights").

In the relativistic BPRM calculations the set of $SL\pi$ are recoupled to obtain (e + ion) levels with total $J\pi$, followed by diagonalisation of the $(N+1)$-electron Hamiltonian,

$$H_{N+1}^{BP}\Psi = E\Psi. \tag{2}$$

The BP Hamiltonian is

$$H_{N+1}^{\mathrm{BP}} = H_{N+1} + H_{N+1}^{\mathrm{mass}} + H_{N+1}^{\mathrm{Dar}} + H_{N+1}^{\mathrm{so}}, \tag{3}$$

where H_{N+1} is the nonrelativistic Hamiltonian,

$$H_{N+1} = \sum_{i=1}^{N+1}\left\{-\nabla_i^2 - \frac{2Z}{r_i} + \sum_{j>i}^{N+1}\frac{2}{r_{ij}}\right\}, \tag{4}$$

and the additional terms are the one-body terms, the mass correction term, the Darwin term and the spin-orbit term respectively. Spin-orbit interaction, H_{N+1}^{so}, splits the LS terms into fine-structure levels labeled by $J\pi$, where J is the total angular momentum. Other terms of the Breit-interaction [22],

$$H^B = \sum_{i>j}[g_{ij}(\mathrm{so}+\mathrm{so}') + g_{ij}(\mathrm{ss}')], \tag{5}$$

representing the two-body spin-spin and the spin-other-orbit interactions are not included.

The positive and negative energy states (Eq. 1) define continuum or bound (e + ion) states,

$$E = k^2 > 0 \longrightarrow \text{continuum (scattering) channel}$$
$$E = -\frac{z^2}{v^2} < 0 \longrightarrow \text{bound state}, \tag{6}$$

where v is the effective quantum number relative to the core level. If $E < 0$ then all continuum channels are 'closed' and the solutions represent bound states. Determination of the quantum defect ($\mu(\ell)$), defined as $v_i = n - \mu(\ell)$ where v_i is relative to the core level $S_iL_i\pi_i$, is helpful in establishing the ℓ-value associated with a given channel (level).

At E < 0 a scattering channel may represent a bound state at the proper eigenvalue of the Hamiltonian (Eq. 2). A large number of channels are considered for the radiative processes of Fe V. Each SLπ or Jπ symmetry is treated independently and corresponds to a large number of channels. Therefore, the overall configuration interaction included in the total (e + ion) wavefunction expansion is quite extensive. This is the main advantage of the CC method in representing electron correlation accurately.

2.1. *Level identification and coupling schemes*

The BPRM calculations in intermediate coupling employ the pair-coupling representation

$$\begin{aligned} S_i + L_i &\longrightarrow J_i, \\ J_i + \ell &\longrightarrow K, \\ K + s &\longrightarrow J, \end{aligned} \tag{7}$$

where the 'i' refers to the target ion level and ℓ, s are the orbital angular momemtum (partial wave) and spin of the additional electron. According to designations of a collision complex, a channel is fully specified by the quantum numbers

$$(S_iL_i\ J_i)\pi_i\ \varepsilon_i\ \ell_i\ Ks\ [J\pi] \tag{8}$$

The main problem in identification of the fine structure levels stems from the fact that the bound levels are initially given

only as eigenvalues of the (e + ion) Hamiltonian of a given symmetry $J\pi$. Each level therefore needs to be associated with the quantum numbers characterizing a given collision channel. Subsequently, three main parameters are to be determined:

(*i*) the parent or the target ion level,
(*ii*) the orbital, effective and principal quantum numbers (l, v, n) of the $(N+1)$th electron, and
(*iii*) the symmetry, $SL\pi$.

The task is relatively straightforward for simple few-electron atomic systems. For example, in a recent work Nahar and Pradhan [11] have calculated a large number of transition probabilities for Li-like Fe XXIV and He-like Fe XXV, where the problem of level identification is trivial, compared to the present work, since the bound levels are well separated in energy and in v. However when a number of mixed bound levels fall within a given interval $(v, v+1)$, for the same $J\pi$, the quantum numbers and the magnitude of the components in all associated channels must be analysed. A scheme for identification of levels is developed (discussed later) that rests mainly on an analysis of quantum defects of the bound levels and their orbital angular momenta, and the percentage of the total wavefunction in all channels of a given $J\pi$.

Following level identification, further work is needed to enable a direct correspondence with standard spectroscopic designations that follow different coupling schemes, such as between LS and JJ, appropriate for atomic structure calculations as, for example, in the NIST tables of observed energy levels [1]. The correspondence provides the check for completeness of calculated set of levels or the levels missing. The level identification procedure involves considerable manipulation of the bound level data and, although it has been encoded for general applications, still requires analysis and interpretation of problem cases of highly mixed levels that are difficult to identify.

2.2 *Oscillator strengths and transition probabilities*

The oscillator strength (or photoionization cross section) is proportional to the generalized line strength defined, in either length form or velocity form, by the equations

$$S_{\rm L} = \left| \left\langle \Psi_f | \sum_{j=1}^{N+1} r_j | \Psi_i \right\rangle \right|^2 \tag{9}$$

and

$$S_{\rm V} = \omega^{-2} \left| \left\langle \Psi_f | \sum_{j=1}^{N+1} \partial\partial r_j | \Psi_i \right\rangle \right|^2 . \tag{10}$$

In these equations ω is the incident photon energy in Rydberg units, and Ψ_i and Ψ_f are the wave functions representing the initial and final states respectively. The boundary conditions satisfied by a bound state with negative energy correspond to exponentially decaying partial waves in all 'closed' channels, whilst those satisfied by a free or continuum state correspond to a plane wave in the direction of the ejected electron momentum $\boldsymbol{k}$ and ingoing waves in all open channels.

Using the energy difference, E_{ji}, between the initial and final states, the oscillator strength, f_{ij}, for the transition can be obtained from S as

$$f_{ij} = \frac{E_{ji}}{3g_i} S, \tag{11}$$

and the Einstein's A-coefficient, A_{ji}, as

$$A_{ji}(\text{a.u.}) = \frac{1}{2}\alpha^3 \frac{g_i}{g_j} E_{ji}^2 f_{ij}, \tag{12}$$

where α is the fine structure constant, and g_i, g_j are the statistical weight factors of the initial and final states, respectively. In terms of c.g.s. unit of time,

$$A_{ji}(\text{s}^{-1}) = \frac{A_{ji}(\text{a.u.})}{\tau_0}, \tag{13}$$

where $\tau_0 = 2.4191^{-17}$ s is the atomic unit of time.

3. Computations

The target wavefunctions of Fe VI were obtained by Chen and Pradhan [21] from an atomic structure calculation using the Breit–Pauli version of the SUPERSTRUCTURE program [22], intended for electron collision calculations with Fe VI using the Breit–Pauli R-matrix method. Present work employs their optimized target of 19 fine structure levels [21] corresponding to the 8-term LS basis set of $3d^3(^4F, ^4P, ^2G, ^2P, ^2D2, ^2H, ^2F, ^2D1)$. The set of correlation configurations used were $3s^23p^63d^24s$, $3s^23p^63d^24d$, $3s3p^63d^4$, $3p^63d^5$, $3s^23p^43d^5$, and $3p^63d^44s$. The values of the scaling parameter in the Thomas–Fermi potential for each orbital of the target ion are given in Ref. [21]. Table I lists the 19 fine structure energy levels of Fe VI used in the eigenfunction expansion where the energies are the observed ones. Most bound levels in low ionization stages correspond to the level of excitation of the parent ion involving the first few excited states. The criterion remains the accuracy of the target represetation that constitute the core ion states. The $(N+1)$ electron configurations, Φ_j, which meet the orthogonality condition for the CC expansion (the second term of the wavefunction, Eq. (1)) are given below Table I. The same set of configurations is used for all the states considered in this work. STG1 of the BPRM codes computes

Table I. *The 19 fine strucuture levels of Fe IV in the close coupling eigenfunction expansion of Fe V. List of configurations, Φ_j, in the second sum of Ψ is given below the table.*

Term	J_t	$E_t(Ryd)$	Term	J_t	$E_t(Ryd)$
$3d^3(^4F)$	3/2	0.0	$3d^3(^2P)$	1/2	0.241445
$3d^3(^4F)$	5/2	0.004659	$3d^3(^2D2)$	5/2	0.259568
$3d^3(^4F)$	7/2	0.010829	$3d^3(^2D2)$	3/2	0.260877
$3d^3(^4F)$	9/2	0.018231	$3d^3(^2H)$	9/2	0.261755
$3d^3(^4P)$	1/2	0.170756	$3d^3(^2H)$	11/2	0.266116
$3d^3(^4P)$	3/2	0.172610	$3d^3(^2F)$	7/2	0.421163
$3d^3(^4P)$	5/2	0.178707	$3d^3(^2F)$	5/2	0.424684
$3d^3(^2G)$	7/2	0.187871	$3d^3(^2D1)$	5/2	0.653448
$3d^3(^2G)$	9/2	0.194237	$3d^3(^2D1)$	3/2	0.656558
$3d^3(^2P)$	3/2	0.238888			

Φ_j:, $3s^23p^63d^4$, $3s^23p^63d^34s$, $3s^23p^63d^34p$, $3s^23p^63d^34d$, $3s^23p^53d^44s$, $3s^23p^53d^44d$, $3s^23p^53d^34s$, $3p^53d^54s4d$, $3p^63d^54p$, $3s^23p^43d^6$, $3s^23p^43d^54p$, $3s3p^63d^34s4d$, $3p^63d^34s4p^2$, $3s^23p^43d^44p^2$, $3s^23p^43d^44s^2$, $3s3p^63d^44s$, $3s^23p^53d^5$, $3p^63d^6$, $3p^63d^34s^24d$, $3s3p^63d^44d$.

the one- and two-electron radial integrals using the one-electron target orbitals generated by SUPERSTRUCTURE. The number of continuum basis functions is 12.

The present calculations are concerned with all possible bound levels with $n \leq 10$, $\ell \leq n-1$. These correspond to total (e + Fe VI) symmetries ($SL\pi$) with $2S+1 = 1, 3, 5$ and $L = 0-10$ (even and odd parities). The intermediate coupling calculations are carried out on recoupling these LS symmetries in a pair-coupling representation, Eq. 6, in stage RECUPD. The computer memory requirement for this stage is the maximum, since it carries out angular algebra of dipole matrix elements of a large number of fine structure levels. The (e + Fe VI) Hamiltonian is diagonalized for each resulting $J\pi$ in STGH. The negative eigenvalues of the Hamiltonian correspond to the bound levels of Fe V, that are found according to the procedure described below.

3.1. *Calculation of bound levels*

The eigenenergies of the Hamiltonian for each $J\pi$ are determined with a numerical search on an effective quantum number mesh, with an interval $\Delta\nu$, using the code STGB. In the relativistic case, the number of Rydberg series of levels increases considerably from those in LS coupling due to splitting of the target states into their fine structure components. This results in a large number of fine structure levels in comparatively narrow energy bands. A mesh with $\Delta(\nu) = 0.01$ is usually adequate to scan for LS term energies; however, it is found to be of insufficient resolution for fine structure energy levels. The mesh needs to be finer by an order of magnitude, i.e., $\Delta(\nu) = 0.001$, so as not to miss out any significant number of bound levels. This considerably increases the computational requirements for the intermediate coupling calculations of bound levels over the LS coupling case by orders of magnitude. The calculations take up to several CPU hours per $J\pi$ in order to determine the corresponding eigenvalues. All bound levels of total $J \leq 8$, of both parities, are considered. However, a further search with an even finer $\Delta\nu$ reveals that a few levels are still missing for some $J\pi$ symmetries.

3.2. *Procedure for level identification*

The energy levels in the BPRM approximation (from STGB) are identified by $J\pi$ alone. This is obviously insufficient information to identify all associated quantum numbers of a level from among a large set of levels for each $J\pi$, typically a few hundred for Fe V. A sample set of energy levels for $J = 2$, even parity, obtained from the BPRM calculations is presented in Table II. The table shows energies and effective quantum number ν_g, as calculated relative to the ground level ($3d^3\,{}^4F_{3/2}$) of the core ion Fe VI. The complexity of the calculations, and that of level identification, may be gauged from the fact that 30 of these levels have nearly the same ν_g. Further, the ν_g does not in general correspond to the actual effective quantum number of the Fe V level since it may belong to an excited parent level, and not the ground level, of Fe VI.

A scheme has been developed to identify the levels with complete spectroscopic information consisting of

$$(C_t\ S_t\ L_t\ J_t\pi_t\ell\ [K]\mathrm{s})\ \ J\ \pi, \tag{14}$$

and also to designate the levels with a possible $SL\pi$ symmetry. The designation of the $SL\pi$, from the identifications denoted above, is generally ambiguous since the collision channels are all in intermediate coupling. However, in most cases we are able to carry through the identification procedure to the LS term designation. An advantage of identification is that it greatly facilitates the completeness check for all possible LS terms and locate any missing levels. A computer code PRCBPID has been developed to identify all the quantum numbers relevant to the $J\pi$ and the LS term assignments. Identification is carried out for all the levels belonging to a $J\pi$ symmetry at a time.

Table II. *Sample set of calculated energy levels (in z^2-scale) of $J = 2$.*

E(Ry)	ν_g	E(Ry)	ν_g
−1.492946E-01	2.58808	−1.455232E-01	2.62140
−1.421287E-01	2.65252	−1.383809E-01	2.68820
−1.381112E-01	2.69083	−1.373195E-01	2.69857
−1.355085E-01	2.71654	−1.307289E-01	2.76576
−1.202324E-01	2.88396	−1.185430E-01	2.90444
−9.421634E-02	3.25789	−9.408765E-02	3.26012
−9.385297E-02	3.26419	−9.375868E-02	3.26584
−9.098725E-02	3.31520	−9.071538E-02	3.32016
−8.971136E-02	3.33869	−8.651911E-02	3.39973
−8.627750E-02	3.40448	−8.536568E-02	3.42262
−8.458038E-02	3.43847	−8.448129E-02	3.44049
−8.420175E-02	3.44619	−8.371297E-02	3.45624
−8.338890E-02	3.46295	−8.317358E-02	3.46743
−8.306503E-02	3.46969	−8.225844E-02	3.48666
−8.180410E-02	3.49633	−8.135593E-02	3.50595
−7.919621E-02	3.55343	−7.827940E-02	3.57418
−7.815480E-02	3.57703	−7.770277E-02	3.58742
−7.708061E-02	3.60186	−7.691196E-02	3.60581
−7.594121E-02	3.62879	−7.370981E-02	3.68330
−7.315088E-02	3.69735	−7.138001E-02	3.74293
−7.028267E-02	3.77204	−6.977748E-02	3.78567
−6.955230E-02	3.79179	−6.845060E-02	3.82218
−6.765945E-02	3.84446	−6.721368E-02	3.85719
−6.518968E-02	3.91661	−6.265635E-02	3.99501
−6.190890E-02	4.01905	−6.111942E-02	4.04492
−5.831623E-02	4.14100		

The components of the total wavefunction of a given fine structure energy level span all closed "collision" channels $(C_tS_tL_t(J_t)\pi_t)\varepsilon l$. Each channel contains the information of the relevant core and the outer electron angular momentum. The "channel weights", mentioned earlier, determine the magnitude of the wavefunction in the outer R-matrix region of each channel evaluated in STGB. A bound level may be readily assigned to the quantum numbers of a given channel provided the corresponding channel weight (in percentage terms) dominates the other channels.

The number of channels can be large especially for complex ions. For Fe V, for example, each level with $J > 2$ corresponds to several hundred channels. As the first step in the level identification scheme we isolate the two most dominant channels by comparing all channel percentage weights. The reason is that the largest channel percentage weight may not uniquely determine the identifications since the channel weights are evaluated from the outer region contributions ($r > a$); the inner region contributions are unknown. Also, many levels are often heavily mixed and no assignment for the dominant channel may be made.

The program, PRCBPID, sorts out the duplicate identifications in all the levels of the $J\pi$ symmetry. Two

levels with the same configuration and set of quantum numbers can actually be two independent levels due to outer electron spin addition/subtraction to/from the parent spin angular momentum, i.e. $S_t \pm s = S$. The identical pair of levels are tagged with positive and negative signs indicating higher and lower multiplicity respectively. The lower energies are normally assigned with the higher spin multiplicity. However, the energies and effective quantum numbers (v) of levels of higher and lower spin multiplicity can be very close to each other, in which case the spin multiplicity assignment may be uncertain.

One important identification criterion is the analysis of the quantum defect, μ, or the effective quantum number, v, of the outer or the valence electron. The principle quantum number, n, of the outer electron of a level is determined from its v, and a Rydberg series of levels can be identified from the effective quantum number. Hence, in the identification procedure, v of the lowest member (level with the lowest principal quantum number of the valence electron) of a Rydberg series is determined from quantum defect analysis of all the computed levels for each partial wave l. The lowest partial wave has the highest quantum defect. A check is maintained to differentiate the quantum defect of a 's' electron with that of an equivalent electron state which has typically a large value in the close coupling calculations. The principle quantum number, n, of the lowest member of the series is determined from the orbital angular momentum of the outer electron and the target or core configuration. Once v and $\mu = n - v$ of the lowest member are known, the n-values of all levels can be assigned for each paritial wave, l. The relevant Rydberg series of levels is also identified from the levels that have the same symmetry, $J\pi$, core configuration, $C_t\ S_t\ L_t\pi_t$ and outer electron orbital angular momentum l, but different v that differs between successive levels by ~ 1. While the $v(n\ \ell)$ are more accurate for the higher members of the series, they are more approximate for the lowest ones. The quantum defect of a given partial wave ℓ also varies slightly with different parent core levels and final SLJ symmetries.

Of the two most dominant channels the proper one for each bound level is determined based on several criteria. There are cases when more than two levels are found to have identical identifications. These levels are checked individually for proper identification. Often a swap of identifications is needed between the two sets of dominant channels since the second dominating channel is more likely to be associated with the given level, consistent with all other criteria. In some cases the most dominant channel (largest percentage weight in the outer region) may correspond to comparatively larger v for the partial wave ℓ, than to a reasonable v for the second channel, indicating that the identification should correspond to the second channel.

In a few cases a level is found not to correspond to any of the two dominant channels, predetermined from the channel weights. At the same time often a level is found to be missing in the same energy range. In such case the level is assigned to a channel of lower percentage weight that has a reasonable core configuration and term, nl quantum numbers for the outer electron and effective quantum number that match the missing level.

There are a number of levels belonging to equivalent- electron configurations and require different identification criteria from those of the Rydberg states. These levels usually have:

(*i*) a number of approximately equal channel weights, and
(*ii*) quantum defects that are larger than that of the lowest partial wave, or an inconsistent v that does not match with any reasonable n.

Once these levels are singled out, they are identified with the possible configurations of the core level, augmented by one electron in the existing orbital sub-shell. These low-lying levels are often assigned to those identified from the small experimentally available set of observed levels. The levels that can not be identified in the above procedure, such as by swapping of channels, or maching to a missing level, are assumed to belong to mixed states. These are not analysed futher by quantum defects.

Two additional (and related) problems, as mentioned above, are addressed in the identification work: (A) standard LS coupling designation, $SL\pi$, and (B) the completeness check for the set of all fine structure components within an LS multiplet. Identification according to collision channel quantum numbers is not quite sufficient to establish a direct correspondence with the standard spectroscopic notation employed in atomic structure calculations, or in the compiled databases such as those by the U.S. National Institute for Standards and Technology (NIST).

The possible set of $SL\pi$s of a level is obtained from the target term, $S_tL_t\pi_t$, and the valence electron angular momentum, l, at the first occurance of the level in the set. The total spin multiplicity of the level is defined according to the energy level position as discussed above. For example, the core $3d^3(^4F^e)$ combining with a 4d electron forms the terms ^{5}(P, D, F, G, H)^e and ^{3}(P, D, F, G, H)^e (Table IV) where the quintet for each L should be lower than the triplet.

To each LS symmetry, $SL\pi$, of the set belongs a set of predetermined J-levels. The set of total J-values of same spin multiplicity is then calculated from all possible LS terms, equal to $|\boldsymbol{L} + \boldsymbol{S}|$. The program sorts out all calculated fine stucture levels with the same configuration, but with different sets of J_t and J, e.g. $(C_tS_tL_tJ_t\pi_tn\ell)\ \ J\pi$ (including the sign for the upper or lower spin multiplicity), compares them with the predetermined set, and groups them together. Thus a correspondence is made between the set of $SL\pi$ and the calculated fine structure levels of same configuration.

In addition to the correspondence between the two sets, the program PRCBPID also calculates the possible set of $SL\pi$'s for each single J-level in above group. In the set of $SL\pi$s, the total spin is fixed while the angular momentum, L, varies. In the above example for the quintets, ^{5}(P, D, F, G, H)^e, each $J = 1$ level is assigned to a possible set of terms, ^{5}(P, D, F) (Table IV).

However, these levels can be futher identified uniquely following Hund's rule that the term with the larger angular momentum, L, is the lower one, i.e., the first or the lowest $J = 1$ level should correspond to ^{5}F, the second one to ^{5}D and the last one to ^{5}P.

The completeness of sets of fine structure levels with respect to the LS terms are checked. As mentioned above, PRCBPID determines the possible sets of $SL\pi$ from the target term and valence electron angular momentum of a level at its first occurrence and calculates the total J-values of

the set of *LS* terms. The number of these *J*-values, *Nlv*, is compared with that of calculated levels, *Ncal* to check the completeness. For example, for the above case of ^{5}(P, D, F, G, H)^e in Table IV discussed above, ^{5}P can have $J = 1, 2, 3$, ^{5}D can have $J = 0, 1, 2, 3, 4$, and so on, giving a total of 23 fine structure levels for this set of *LS* terms. The one $J = 0$ level belongs to ^{5}D, the three $J = 1$ levels belong to ^{5}(P, D, F), and so on. All 23 levels of this set are found in the computed levels (Table IV), thus making the computed set complete. This procedure, in addition to finding the link between the two diiferent coupling schemes, enables an independent counting of the number of levels obtained, and ascertains missing or mis-identified levels.

3.3 *Transition probabilities*

The oscillator strengths (*f*-values) and transition probabilites (*A*-values) for bound-bound fine structure level transitions in Fe V are calculated for levels up to $J \leq 8$. Computations are carried out using STGBB of the BPRM codes.

The *f*-values are initially calculated by the program STGBB with level designations given by $J\pi$ only. However, the transitions may be fully described following the level identifications as described in the previous section. Work is in progress to identify all the transitions with proper quantum numbers, configurations and possible $SL\pi$'s.

A subset of the large number of transitions has been processed with complete identifications. Among these transitions are those that correspond to the experimentally observed levels [23]. As these levels have been identified, their oscillator strenghts could be sorted out from the file of *f*-values. Another subsidiary code, PRCBPRAD, is developed to reprocess the transition probabilities where the calculated transition energies are replaced by the observed ones for improved accuracy.

The computation time required for the BPRM calculations was orders of magnitude longer compared to oscillator strengths calculations in *LS* coupling, as carried out under the OP for example. The time excludes that needed for creating the necessary bound state wavefunctions and calculating dipole matrix elements using the R-matrix package of codes. Computations are carried out for one or a few pairs of symmetries at a time requiring several hours of CPU time on the Cray T94. The memory requirement was over 30 MWords.

4. Results and discussion

Theoretical spectroscopic data are calculated on a large-scale with relativistic fine structure included in an *ab initio* manner, and ensuring completeness in terms of obtaining nearly all possible energy levels and transition probabilities for Fe V for the total angular symmetries considered. The results are described below.

4.1. *Energy levels*

We have calculated 3,865 fine structure bound levels, with $0 \leq J \leq 8$, for Fe V. Following level identification, as explained in the previous section, the energy levels are arranged according to ascending order in energy.

The present energies are compared with the relatively small set of experimentally observed levels compiled by NIST [23] in Table III. All 179 observed levels are obtained and identified. Asterisks attached to levels in Table III indicate an incomplete set of observed levels corresponding to the *LS* term. Often in experimental measurements the weak lines are not observed. The theoretical datasets on the other hand are usually complete.

We find some discrepancies regarding the identification of a couple of levels in the NIST tabulation. The $J = 2$ level at 2.9395 Ry identified in the NIST table as $3d^3(^4P)4p(^5S^o)_2$, from the maximum leading percentage, may have been misidentified. Present analysis for the completeness of a set of fine structure levels belonging to a term indicates it as an extra level for the given configuration and that the possible *LS* terms for this level are $3d^3(^2D2)4p(^3PDF^o)$, possibly $^3F^o$. Similarly the NIST identification for the $J = 3$ level at 2.8968 Ry is $3d^3(^2P)4p(^3D^o)_3$, from the maximum leading percentage. Present calculations however assign the level to possible LS terms, $3d^3(^2D2)4p(^3DF^o)$, and most likely to $^3D^o$.

In the computed set of fine structure levels the observed levels are usually the ones with the lowest energy in each subset of $J\pi$. The lowest calculated levels are the 34 levels of the ground configuration $3d^4$ of Fe V, in agreement with the observed ones. The agreement between the observed and calculated energies for these levels is within 1%. The calculated energies agree to about 1% with the measured ones for most of the observed levels. Although the energies are exoected to be highly accurate, but the uncertainty in the calculations is not comparable to that in spectroscopic observations (of the order of few wavenumbers).

Employing the completeness procedure the computed fine structure levels are tabulated, according to the two sets of cross-correlating quantum numbers: one according to the collision channels identified as $(C_t S_t\ L_t\ J_t \pi_t n\ell[K]s)$ $J\pi$, and the other according to the complete set of *J*-values for each multiplicity $(2S + 1)$, *L* and π. A subset of the complete table of fine structure levels is presented in Table IV. (The complete table will be available electronically). Each set of levels is grouped by the possible set of *LS* terms followed by the levels of same configuration, core term, total spin multiplicity and parity, and with different *J*-values. The header for each group contains the total number of possible *J*-levels, *Nlv*, total spin multiplicity, parity, and all possible *L* values formed from the core and the outer electron. The possible *J*-values for each $SL\pi$ are given within parentheses next to each *L* value.

The two sets of quantum numbers are compared. The levels that may be missing or mis-identified are thereby checked out. The number of computed levels, *Ncal*, is compared with that expected from angular and spin couplings, *Nlv*. For most of the configurations the set of levels is complete except for the high lying ones. The comparison detects missing levels. An example is shown in the the set of $3d^32(^2D)5d^3$(S, P, D, F, G)^e in Table IV where one level with $J^e = 4$ is missing.

In Table IV, the effective quantum number *v* is specified alongwith other quantum numbers for each level. The consistency in $v = (z/\sqrt{(E - E_t)})$, where E_t is the corresponding target energy, for each set of levels may be noted.

Table III. *Comparison of calculated and observed energy levels of Fe V.*

Configuration	Term	J	E(cal)	E(expt)
$3d^4$	^5D	4.0	5.5493	5.5015
$3d^4$	^5D	3.0	5.5542	5.5058
$3d^4$	^5D	2.0	5.5580	5.5094
$3d^4$	^5D	1.0	5.5607	5.5119
$3d^4$	^5D	0.0	5.5621	5.5132
$3d^42$	^3P	2.0	5.3247	5.2720
$3d^42$	^3P	1.0	5.3389	5.2856
$3d^42$	^3P	0.0	5.3471	5.2940
$3d^4$	^3H	6.0	5.3074	5.2805
$3d^4$	^3H	5.0	5.3111	5.2833
$3d^4$	^3H	4.0	5.3143	5.2860
$3d^42$	^3F	4.0	5.3043	5.2674
$3d^42$	^3F	3.0	5.3064	5.2686
$3d^42$	^3F	2.0	5.3076	5.2693
$3d^4$	^3G	5.0	5.2581	5.2359
$3d^4$	^3G	4.0	5.2614	5.2384
$3d^4$	^3G	3.0	5.2651	5.2415
$3d^4$	^1G	4.0	5.2006	5.1798
$3d^4$	^3D	3.0	5.1950	5.1794
$3d^4$	^3D	2.0	5.1945	5.1782
$3d^4$	^3D	1.0	5.1928	5.1767
$3d^4$	^1I	6.0	5.1852	5.1713
$3d^42$	^1S	0.0	5.1700	5.1520
$3d^42$	^1D	2.0	5.1353	5.0913
$3d^4$	^1F	3.0	5.0476	5.0326
$3d^41$	^3P	2.0	4.9756	4.9495
$3d^41$	^3P	1.0	4.9663	4.9398
$3d^41$	^3P	0.0	4.9616	4.9352
$3d^41$	^3F	4.0	4.9719	4.9460
$3d^41$	^3F	3.0	4.9706	4.9449
$3d^41$	^3F	2.0	4.9712	4.9453
$3d^41$	^1G	4.0	4.8830	4.8636
$3d^41$	^1D	2.0	4.6609	4.6581
$3d^41$	^1S	0.0	4.4302	4.4093
$3d^3(^4F)4s$	^5F	5.0	3.7161	3.7964
$3d^3(^4F)4s$	^5F	4.0	3.7228	3.8025
$3d^3(^4F)4s$	^5F	3.0	3.7282	3.8077
$3d^3(^4F)4s$	^5F	2.0	3.7324	3.8116
$3d^3(^4F)4s$	^5F	1.0	3.7352	3.8143
$3d^3(^4F)4s$	^3F	4.0	3.6222	3.7194
$3d^3(^4F)4s$	^3F	3.0	3.6311	3.7277
$3d^3(^4F)4s$	^3F	2.0	3.6381	3.7344
$3d^3(^4P)4s$	^5P	3.0	3.5483	3.6402
$3d^3(^4P)4s$	^5P	2.0	3.5532	3.6453
$3d^3(^4P)4s$	^5P	1.0	3.5554	3.6475
$3d^3(^2G)4s$	^3G	5.0	3.5090	3.6038
$3d^3(^2G)4s$	^3G	4.0	3.5130	3.6076
$3d^3(^2G)4s$	^3G	3.0	3.5158	3.6101
$3d^3(^4P)4s$	^3P	2.0	3.4595	3.5663
$3d^3(^4P)4s$	^3P	1.0	3.4677	3.5738
$3d^3(^4P)4s$	^3P	0.0	3.4706	3.5763
$3d^3(^2G)4s$	^1G	4.0	3.4636	3.5673
$3d^3(^2P)4s$	^3P	2.0*	3.4528	3.5583
$3d^3(^2P)4s$	^3P	1.0*	3.4515	3.5575
$3d^3(^2D2)4s$	^3D	3.0	3.4337	3.5399
$3d^3(^2D2)4s$	^3D	2.0	3.4330	3.5394
$3d^3(^2D2)4s$	^3D	1.0	3.4405	3.5468
$3d^3(^2H)4s$	^3H	6.0	3.4364	3.5346
$3d^3(^2H)4s$	^3H	5.0	3.4392	3.5370
$3d^3(^2H)4s$	^3H	4.0	3.4398	3.5377
$3d^3(^2P)4s$	^1P	1.0	3.4015	3.5131
$3d^3(^2D2)4s$	^1D	2.0	3.3877	3.5027
$3d^3(^2H)4s$	^1H	5.0	3.3894	3.4965
$3d^3(^2F)4s$	^3F	4.0	3.2711	3.3841
$3d^3(^2F)4s$	^3F	3.0	3.2695	3.3822
$3d^3(^2F)4s$	^3F	2.0	3.2682	3.3806
$3d^3(^2F)4s$	^1F	3.0	3.2280	3.3468
$3d^3(^4F)4p$	$^5G^o$	6.0	3.1534	3.1594
$3d^3(^4F)4p$	$^5G^o$	5.0	3.1631	3.1700
$3d^3(^4F)4p$	$^5G^o$	4.0	3.1710	3.1787
$3d^3(^4F)4p$	$^5G^o$	3.0	3.1773	3.1858
$3d^3(^4F)4p$	$^5G^o$	2.0	3.1821	3.1912
$3d^3(^4F)4p$	$^5F^o$	1.0*	3.4015	3.1644
$3d^3(^4F)4p$	$^5D^o$	4.0	3.1359	3.1498
$3d^3(^4F)4p$	$^5D^o$	3.0	3.1433	3.1559
$3d^3(^4F)4p$	$^5D^o$	2.0	3.1479	3.1609
$3d^3(^4F)4p$	$^5D^o$	1.0	3.1408	3.1540
$3d^3(^4F)4p$	$^5D^o$	0.0	3.1469	3.1565
$3d^3(^2D1)4s$	^3D	3.0	3.0074	3.1581
$3d^3(^2D1)4s$	^3D	2.0	3.0058	3.1564
$3d^3(^2D1)4s$	^3D	1.0	3.0047	3.1551
$3d^3(^4F)4p$	$^5F^o$	5.0*	3.1191	3.1343
$3d^3(^4F)4p$	$^5F^o$	4.0*	3.1243	3.1391
$3d^3(^4F)4p$	$^5F^o$	3.0*	3.1300	3.1443
$3d^3(^4F)4p$	$^5F^o$	2.0*	3.135	3.1496
$3d^3(^4F)4p$	$^3D^o$	3.0	3.117	3.1331
$3d^3(^4F)4p$	$^3D^o$	2.0	3.1258	3.1401
$3d^3(^4F)4p$	$^3D^o$	1.0	3.1309	3.1439
$3d^3(^2D1)4s$	^1D	2.0	2.9636	3.1210
$3d^3(^4F)4p$	$^3G^o$	5.0	3.0737	3.0973
$3d^3(^4F)4p$	$^3G^o$	4.0	3.0812	3.1035
$3d^3(^4F)4p$	$^3G^o$	3.0	3.0872	3.1083
$3d^3(^4F)4p$	$^3F^o$	4.0	3.0449	3.0716
$3d^3(^4F)4p$	$^3F^o$	3.0	3.0520	3.0779
$3d^3(^4F)4p$	$^3F^o$	2.0	3.0586	3.0836
$3d^3(^4P)4p$	$^5P^o$	3.0	2.9842	3.0078
$3d^3(^4P)4p$	$^5P^o$	2.0	2.9903	3.0151
$3d^3(^4P)4p$	$^5P^o$	1.0	2.9937	3.0195
$3d^3(^4P)4p$	$^5D^o$	4.0	2.9655	2.9792
$3d^3(^4P)4p$	$^5D^o$	3.0	2.9600	2.9883
$3d^3(^4P)4p$	$^5D^o$	2.0	2.9733	2.9912
$3d^3(^4P)4p$	$^5D^o$	1.0	2.9747	3.0058
$3d^3(^4P)4p$	$^5D^o$	0.0	2.9797	3.0094
$3d^3(^4P)4p$	$^3P^o$	2.0	2.9622	3.0038
$3d^3(^4P)4p$	$^3P^o$	1.0	2.9635	2.9911
$3d^3(^4P)4p$	$^3P^o$	0.0	2.9676	2.9941
$3d^3(^2G)4p$	$^3H^o$	6.0	2.9484	2.9739
$3d^3(^2G)4p$	$^3H^o$	5.0	2.9591	2.9863
$3d^3(^2G)4p$	$^3H^o$	4.0	2.9526	2.9942
$3d^3(^2G)4p$	$^3G^o$	5.0	2.9289	2.9613
$3d^3(^2G)4p$	$^3G^o$	4.0	2.9353	2.9662
$3d^3(^2G)4p$	$^3G^o$	3.0	2.9412	2.9726
$3d^3(^2G)4p$	$^3F^o$	4.0	2.9238	2.9583
$3d^3(^2G)4p$	$^3F^o$	3.0	2.9262	2.9540
$3d^3(^2G)4p$	$^3F^o$	2.0	2.9329	2.9567
$3d^3(^2P)4p$	$^3P^o$	1.0	2.9326	2.9439
$3d^3(^2P)4p$	$^3P^o$	0.0	2.9458	2.9413
$3d^3(^2G)4p$	$^1G^o$	4.0	2.9068	2.9430
$3d^3(^4P)4p$	$^5S^o$!	2.0	2.9231	2.9395
$3d^3(^2G)4p$	$^1F^o$	3.0	2.9067	2.9382
$3d^3(^4P)4p$	$^5S^o$	2.0	2.8995	2.9379
$3d^3(^2P)4p$	$^3P^o$	2.0	2.8605	2.8668
$3d^3(^2G)4p$	$^1H^o$	5.0	2.9006	2.9354
$3d^3(^2P)4p$	$^3D^o$	3.0	2.8895	2.9117
$3d^3(^2P)4p$	$^3D^o$	2.0	2.8944	2.9169
$3d^3(^2P)4p$	$^3D^o$	1.0	2.8790	2.9274
$3d^3(^2H)4p$	$^3H^o$	6.0	2.8793	2.9143
$3d^3(^2H)4p$	$^3H^o$	5.0	2.8830	2.9180
$3d^3(^2H)4p$	$^3H^o$	4.0	2.8834	2.9189
$3d^3(^2D2)4p$	$^1P^o$	1.0	2.9031	2.9073
$3d^3(^2D2)4p$	$^3F^o$	4.0*	2.8653	2.8922
$3d^3(^2D2)4p$	$^3F^o$	2.0*	2.9144	2.9055
$3d^3(^2P)4p$	$^3S^o$	1.0	2.8621	2.9052
$3d^3(^4P)4p$	$^3D^o$	3.0	2.8593	2.9030
$3d^3(^4P)4p$	$^3D^o$	2.0	2.8749	2.8991
$3d^3(^4P)4p$	$^3D^o$	1.0	2.8478	2.8991
$3d^3(^2P)4p$	$^3D^o$!	3.0*	2.8718	2.8968
$3d^3(^2H)4p$	$^3I^o$	7.0	2.8414	2.8780
$3d^3(^2H)4p$	$^3I^o$	6.0	2.8487	2.8872

Table III. *continued.*

Configuration	Term	J	E(cal)	E(expt)
$3d^3(^2H)4p$	$^3I^o$	5.0	2.8537	2.8938
$3d^3(^2D2)4p$	$^3D^o$	3.0	2.8366	2.8713
$3d^3(^2D2)4p$	$^3D^o$	2.0	2.8325	2.8761
$3d^3(^2D2)4p$	$^3D^o$	1.0	2.8842	2.8826
$3d^3(^2H)4p$	$^1G^o$	4.0	2.8325	2.8746
$3d^3(^2H)4p$	$^1H^o$	5.0	2.8244	2.8696
$3d^3(^2D2)4p$	$^3P^o$	1.0*	2.8313	2.8652
$3d^3(^2D2)4p$	$^3P^o$	0.0*	2.8300	2.8623
$3d^3(^2D2)4p$	$^1F^o$	3.0	2.8238	2.8593
$3d^3(^2H)4p$	$^3G^o$	5.0	2.8039	2.8496
$3d^3(^2H)4p$	$^3G^o$	4.0	2.8035	2.8483
$3d^3(^2H)4p$	$^3G^o$	3.0	2.8049	2.8476
$3d^3(^2H)4p$	$^1I^o$	6.0	2.8012	2.8489
$3d^3(^4P)4p$	$^3S^o$	1.0	2.7705	2.8282
$3d^3(^2D2)4p$	$^1D^o$	2.0	2.7815	2.8184
$3d^3(^2P)4p$	$^1P^o$	1.0	2.7822	2.8161
$3d^3(^2F)4p$	$^3F^o$	4.0	2.7083	2.7556
$3d^3(^2F)4p$	$^3F^o$	3.0	2.7105	2.7577
$3d^3(^2F)4p$	$^3F^o$	2.0	2.7109	2.7585
$3d^3(^2F)4p$	$^3G^o$	5.0	2.6652	2.7150
$3d^3(^2F)4p$	$^3G^o$	4.0	2.6672	2.7190
$3d^3(^2F)4p$	$^3G^o$	3.0	2.6695	2.7229
$3d^3(^2F)4p$	$^3D^o$	3.0	2.6648	2.7129
$3d^3(^2F)4p$	$^3D^o$	2.0	2.6705	2.7050
$3d^3(^2F)4p$	$^3D^o$	1.0	2.6559	2.7003
$3d^3(^2F)4p$	$^1D^o$	2.0	2.6592	2.7097
$3d^3(^2F)4p$	$^1G^o$	4.0	2.6165	2.6775
$3d^3(^2F)4p$	$^1F^o$	3.0	2.6172	2.6742
$3d^3(^2D1)4p$	$^3D^o$	3.0	2.4918	2.5249
$3d^3(^2D1)4p$	$^3D^o$	2.0	2.4938	2.5278
$3d^3(^2D1)4p$	$^3D^o$	1.0	2.4936	2.5285
$3d^3(^2D1)4p$	$^1D^o$	2.0	2.4581	2.5074
$3d^3(^2D1)4p$	$^3F^o$	4.0	2.4499	2.4876
$3d^3(^2D1)4p$	$^3F^o$	3.0	2.4532	2.4935
$3d^3(^2D1)4p$	$^3F^o$	2.0	2.4510	2.4938
$3d^3(^2D1)4p$	$^3P^o$	2.0	2.4196	2.4649
$3d^3(^2D1)4p$	$^3P^o$	1.0	2.4141	2.4580
$3d^3(^2D1)4p$	$^3P^o$	0.0	2.4116	2.4546
$3d^3(^2D1)4p$	$^1F^o$	3.0	2.4058	2.4518
$3d^3(^2D1)4p$	$^1P^o$	1.0	2.3394	2.3924

The possible $SL\pi$s for each level are given in the last column. The levels with a single possible term only are uniquely defined. However, those with two or multiple term assignments can be defined uniquely applying Hund's rule that the higher L corresponds to the lower energy of same $J\pi$ as explained in the previous section (we note that Hund's rule may not always apply in cases of strong CI).

There are 112 levels of odd parity that we could not properly identify. Some of these levels are given in Table IV. These levels could be equivalent electron levels of configuration, $3p^5(^2P^o)3d^5$. The 16 LS terms of $3d^5$, which are ^{2}D1, ^{2}P3, ^{2}D3, ^{2}F3, ^{2}G3, ^{2}H3, ^{4}P5, ^{4}F5, ^{2}S5, ^{2}D5, ^{2}F5, ^{2}G5, ^{2}I5, ^{4}D5, ^{4}G5, and ^{6}S5, in combination with the parent core $^2P^o$, form 88 LS terms with 31 singlets, 43 triplets, 13 quintets and 1 septet. The number of fine structure levels from these terms exceed the 112 computed levels that have not been identified.

This new procedure of cross-correlation between two coupling schemes thus provides a powerful check on the completeness and level identification, and is expected to be of use in further BPRM work on complex atomic systems.

4.2. *Transition Probabilities*

The oscillator strengths (f-values) and transition probabilites (A-values) for fine structure level transitions in Fe V are obtained for $J \leq 8$. The allowed $\Delta J = 0, \pm 1$ transitions include both the dipole allowed ($\Delta S = 0, \pm 1$) and the intercombination ($\Delta S \neq 0$) transitions. The total number of computed transition probabilities is well over a million, approximately 1.46×10^6. For most allowed pairs of $J\pi$ symmetries, there are about $10^3 - 10^5$ transitions.

As explained in the previous section, a subset of the encoded transitions have been processed to present them with proper identifications. These correspond to the levels that have been observed. A sample of these is presented in Table V. In all of the f-values presented the calculated transition energy has been replaced by the observed one, using the BPRM line strengths (S) which are energy independent. Since measured energies in general have smaller uncertainties than the calculated ones, this replacement improves the accuracy of the oscillator strengths. The transitions among the 179 observed levels correspond to 3727 oscillator strengths. (The complete set of transition probabilities will be available electronically.)

The f-values in Table V have been reordered to group the transitions of the same multiplet together. This enables a check on the completeness of the set of transitions. As this table corresponds to transitions among observed levels only, the completeness depends on the set of observed levels belonging to the LS terms. For the dipole allowed transitions, the LS multiplets are also given at the end of jj' transitions.

To our knowledge, no measured f-values for Fe V are available for comparison. Current NIST compilation [1] contains no f-values for any allowed transition. On the other hand, Fe V oscillator strengths for a large number of transitions were obtined in the close coupling approximation under the OP [24] and the IP [25]. Both of these datasets are non-relativistic calculations in LS coupling and do not compute fine structure transitions. Fawcett has [26] carried out semi-empirical relativistic atomic structure calculations for fine structure transitions in Fe V. Comparison of the present f-values is made with the previous ones in Table VI, showing various degrees of agreement. Present values agree within 10% with those by Fawcett for a number of fine structure transitions of multiplets, $3d^4(^5D) \rightarrow 3d^3(^4F)4p(^5D^o)$, and $3d^4(^5D) \rightarrow 3d^3(^4P)4p(^5P^o)$, and the disagreement is large with other as well as with those of $3d^4(^5D) \rightarrow 3d^3(^4F)4p(^5F^o)$. The agreement of the present LS multiplets with the others is good for transitions $3d^4(^5D) \rightarrow 3d^3(^4F)4p(^5F^o, ^5D^o, ^5P^o)$. More detailed comparisons will be made at the completion of this work.

The procedure of substitution of experimental for calculated energies provides an indication of uncertainties in the calculated f-values. The difference between the f-values obtained using the calculated transition energies and the observed ones is only a few percents ($< 5\%$) for most of the allowed transitions. The difference is usually larger for the intercombination transitions which have lower transition probabilities. In atomic structure calculations, it is possible to re-adjust eigenenergies of the Hamiltonian to match the observed ones and then use the wavefunctions to obtain the transition probabilities. Such a re-adjustment

Table IV. *Sample table of calculated and identified fine strucuture energy levels of Fe V. Nlv=total number of levels expected for the possible LS terms (specified as 2S+1, π, and set of L with J-values within paratheses), formed from the target term and l of the outer electron, and Ncal = number of calculated levels. SLπ in last column = possible LS terms for each level. Full version available at: http://www.physica.org/digidata/v061p06a00675/tables/tableIV.pdf.*

C_t	$S_tL_t\pi_t$	J_t	nl	J	$E(cal)$	v	$SL\pi$
$Nlv = 5, 5,$ e : F(54321)							
3d3	(4Fe)	3/2	4s	1	−3.73515E+00	2.59	5 F e
3d3	(4Fe)	5/2	4s	2	−3.73238E+00	2.59	5 F e
3d3	(4Fe)	5/2	4s	3	−3.72820E+00	2.59	5 F e
3d3	(4Fe)	7/2	4s	4	−3.72275E+00	2.59	5 F e
3d3	(4Fe)	9/2	4s	5	−3.71610E+00	2.59	5 F e
$Ncal = 5$: set complete $Nlv = 3, 3, e$: $F(432)$							
3d3	(4Fe)	3/2	4s	2	−3.63808E+00	2.62	3 F e
3d3	(4Fe)	7/2	4s	3	−3.63107E+00	2.62	3 F e
3d3	(4Fe)	9/2	4s	4	−3.62225E+00	2.62	3 F e
$Ncal = 3$: set complete $Nlv = 3, 1,$ o:							
P (1) D (2) F (3)							
3d3 1	(2De)	3/2	4p	2	−2.45812E+00	2.83	1 D o
3d3 1	(2De)	5/2	4p	3	−2.40581E+00	2.86	1 F o
3d3 1	(2De)	5/2	4p	1	−2.33944E+00	2.89	1 P o
$Ncal = 3$: set complete $Nlv = 23, 5,$ e:							
P (3 2 1) D (4 3 2 1 0) F (5 4 3 2 1) G (6 5 4 3 2) H (7 6 5 4 3)							
3d3	(4Fe)	3/2	4d	3	−2.37021E+00	3.25	5 PDFGH e
3d3	(4Fe)	5/2	4d	4	−2.36647E+00	3.25	5 DFGH e
3d3	(4Fe)	5/2	4d	5	−2.36189E+00	3.25	5 FGH e
3d3	(4Fe)	3/2	4d	1	−2.35988E+00	3.25	5 PDF e
3d3	(4Fe)	7/2	4d	6	−2.35651E+00	3.25	5 GH e
3d3	(4Fe)	5/2	4d	2	−2.35541E+00	3.26	5 PDFG e
3d3	(4Fe)	9/2	4d	7	−2.35041E+00	3.25	5 H e
3d3	(4Fe)	5/2	4d	1	−2.34932E+00	3.26	5 PDF e
3d3	(4Fe)	9/2	4d	3	−2.34736E+00	3.25	5 PDFGH e
3d3	(4Fe)	7/2	4d	2	−2.34633E+00	3.26	5 PDFG e
3d3	(4Fe)	3/2	4d	2	−2.34397E+00	3.27	5 PDFG e
3d3	(4Fe)	7/2	4d	4	−2.34329E+00	3.26	5 DFGH e
3d3	(4Fe)	5/2	4d	3	−2.34092E+00	3.26	5 PDFGH e
3d3	(4Fe)	9/2	4d	3	−2.33989E+00	3.26	5 PDFGH e
3d3	(4Fe)	9/2	4d	5	−2.33822E+00	3.26	5 FGH e
3d3	(4Fe)	7/2	4d	5	−2.33234E+00	3.27	5 FGH e
3d3	(4Fe)	9/2	4d	6	−2.32699E+00	3.26	5 GH e
3d3	(4Fe)	3/2	4d	4	−2.28772E+00	3.31	5 DFGH e
3d3	(4Fe)	3/2	4d	0	−2.28673E+00	3.31	5 D e
3d3	(4Fe)	7/2	4d	1	−2.28265E+00	3.30	5 PDF e
3d3	(4Fe)	9/2	4d	2	−2.27468E+00	3.30	5 PDFG e
3d3	(4Fe)	7/2	4d	3	−2.26346E+00	3.31	5 PDFGH e
3d3	(4Fe)	9/2	4d	4	−2.25835E+00	3.31	5 DFGH e
$Ncal = 23$: set complete $Nlv = 15, 3,$ e:							
P (2 1 0) D (3 2 1) F (4 3 2) G (5 4 3) H (6 5 4)							
3d3	(4Fe)	3/2	4d	1	−2.35634E+00	3.26	3 PD e
3d3	(4Fe)	5/2	4d	2	−2.35219E+00	3.25	3 PDF e
3d3	(4Fe)	7/2	4d	3	−2.34872E+00	3.25	3 DFG e
3d3	(4Fe)	5/2	4d	4	−2.33701E+00	3.27	3 FGH e
3d3	(4Fe)	5/2	4d	5	−2.28113E+00	3.31	3 GH e
3d3	(4Fe)	3/2	4d	3	−2.28060E+00	3.31	3 DFG e
3d3	(4Fe)	7/2	4d	4	−2.27417E+00	3.31	3 FGH e
3d3	(4Fe)	9/2	4d	6	−2.27323E+00	3.30	3 H e
3d3	(4Fe)	3/2	4d	2	−2.26789E+00	3.32	3 PDF e
3d3	(4Fe)	7/2	4d	5	−2.26632E+00	3.31	3 GH e
3d3	(4Fe)	5/2	4d	0	−2.24585E+00	3.33	3 P e
3d3	(4Fe)	5/2	4d	1	−2.24483E+00	3.33	3 PD e
3d3	(4Fe)	7/2	4d	2	−2.24278E+00	3.33	3 PDF e
3d3	(4Fe)	7/2	4d	3	−2.23973E+00	3.33	3 DFG e
3d3	(4Fe)	9/2	4d	4	−2.23571E+00	3.33	3 FGH e

Table IV. *Continued*

C_t	$S_tL_t\pi_t$	J_t	nl	J	$E(cal)$	v	$SL\pi$
Ncal = 15 : set complete *Nlv* = 13, 5, e:							
P (3 2 1) D (4 3 2 1 0) F (5 4 3 2 1)							
3d3	(4Pe)	1/2	4d	1	−2.16405E+00	3.27	5 PDF e
3d3	(4Pe)	3/2	4d	2	−2.16298E+00	3.27	5 PDF e
3d3	(4Pe)	3/2	4d	3	−2.16165E+00	3.27	5 PDF e
3d3	(4Pe)	3/2	4d	1	−2.15901E+00	3.27	5 PDF e
3d3	(4Pe)	3/2	4d	4	−2.15825E+00	3.27	5 DF e
3d3	(4Pe)	5/2	4d	2	−2.15694E+00	3.27	5 PDF e
3d3	(4Pe)	5/2	4d	3	−2.15521E+00	3.27	5 PDF e
3d3	(4Pe)	5/2	4d	5	−2.15477E+00	3.27	5 F e
Nlv = 13, 5, e:							
P (3 2 1) D (4 3 2 1 0) F (5 4 3 2 1)							
3d3	(4Pe)	1/2	4d	3	−2.13511E+00	3.29	5 PDF e
3d3	(4Pe)	5/2	4d	1	−2.13294E+00	3.29	5 PDF e
3d3	(4Pe)	1/2	4d	2	−2.11203E+00	3.31	5 PDF e
3d3	(4Pe)	5/2	4d	4	−2.09728E+00	3.31	5 DF e
3d3	(4Pe)	3/2	4d	0	−2.08337E+00	3.33	5 D e
Ncal = 13 : set complete *Nlv* = 9, 3, e:							
P (2 1 0) D (3 2 1) F (4 3 2)							
3d3	(4Pe)	5/2	4d	2	−2.13414E+00	3.29	3 PDF e
3d3	(4Pe)	3/2	4d	3	−2.10788E+00	3.31	3 DF e
3d3	(4Pe)	3/2	4d	1	−2.08179E+00	3.33	3 PD e
3d3	(4Pe)	5/2	4d	2	−2.07934E+00	3.46	3 PDF e
3d3	(4Pe)	5/2	4d	1	−2.07801E+00	3.33	3 PD e
3d3	(4Pe)	5/2	4d	3	−2.07780E+00	3.33	3 DF e
3d3	(4Pe)	5/2	4d	0	−2.07641E+00	3.33	3 P e
3d3	(4Pe)	5/2	4d	4	−2.07512E+00	3.33	3 F e
3d3	(4Pe)	3/2	4d	2	−2.04510E+00	3.36	3 PDF e
Ncal = 9 : set complete *Nlv* = 15, 3, e:							
D (3 2 1) F (4 3 2) G (5 4 3) H (6 5 4) I (7 6 5)							
3d3	(2Ge)	7/2	4d	3	−2.16065E+00	3.26	3 DFG e
3d3	(2Ge)	7/2	4d	5	−2.15935E+00	3.26	3 GHI e
3d3	(2Ge)	7/2	4d	6	−2.15443E+00	3.27	3 HI e
3d3	(2Ge)	7/2	4d	4	−2.15035E+00	3.27	3 FGH e
3d3	(2Ge)	9/2	4d	7	−2.14872E+00	3.27	3 I e
3d3	(2Ge)	9/2	4d	3	−2.14865E+00	3.27	3 DFG e
3d3	(2Ge)	9/2	4d	5	−2.14663E+00	3.27	3 GHI e
3d3	(2Ge)	9/2	4d	5	−2.13490E+00	3.28	3 GHI e
3d3	(2Ge)	9/2	4d	6	−2.13050E+00	3.30	3 HI e
3d3	(2Ge)	9/2	4d	2	−2.11451E+00	3.29	3 DF e
3d3	(2Ge)	7/2	4d	1	−2.10743E+00	3.30	3 D e
3d3	(2Ge)	7/2	4d	2	−2.10505E+00	3.30	3 DF e
3d3	(2Ge)	7/2	4d	3	−2.09600E+00	3.31	3 DFG e
3d3	(2Ge)	9/2	4d	4	−2.08773E+00	3.31	3 FGH e
3d3	(2Ge)	9/2	4d	4	−1.95461E+00	3.41	3 FGH e
Ncal = 15 : set complete *Nlv* = 5, 1, e:							
D (2) F (3) G (4) H (5) I (6)							
3d3	(2Ge)	7/2	4d	5	−2.15108E+00	3.27	1 H e
3d3	(2Ge)	7/2	4d	4	−2.13926E+00	3.27	1 G e
3d3	(2Ge)	9/2	4d	3	−2.11077E+00	3.29	1 F e
3d3	(2Ge)	7/2	4d	6	−2.10182E+00	3.27	1 I e
3d3	(2Ge)	7/2	4d	2	−2.09282E+00	3.30	1 D e
Ncal = 5 : set complete *Nlv* = 9, 3, e:							
P (2 1 0) D (3 2 1) F (4 3 2)							
3d3	(2Pe)	1/2	4d	1	−2.11449E+00	3.26	3 PD e
3d3	(2Pe)	3/2	4d	4	−2.10214E+00	3.27	3 F e
3d3	(2Pe)	1/2	4d	2	−2.08472E+00	3.28	3 PDF e
3d3	(2Pe)	1/2	4d	3	−2.08116E+00	3.28	3 DF e
3d3	(2Pe)	3/2	4d	2	−2.07662E+00	3.29	3 PDF e
3d3	(2Pe)	3/2	4d	3	−2.05165E+00	3.30	3 DF e
3d3	(2Pe)	3/2	4d	0	−1.94013E+00	3.39	3 P e
3d3	(2Pe)	3/2	4d	1	−1.93293E+00	3.39	3 PD e
3d3	(2Pe)	3/2	4d	2	−1.89853E+00	3.42	3 PDF e

Table IV. *Continued.*

C_t	$S_tL_t\pi_t$	J_t	nl	J	$E(cal)$	v	$SL\pi$
$Ncal = 9$: set complete $Nlv = 3, 1$, e:							
P (1) D (2) F (3)							
3d3	(2Pe)	3/2	4d	1	−2.08815E+00	3.26	1 P e
3d3	(2Pe)	1/2	4d	2	−1.95699E+00	3.41	1 D e
3d3	(2Pe)	3/2	4d	3	−1.94667E+00	3.38	1 F e
$Ncal = 3$: set complete $Nlv = 5, 1$, e:							
S (0) P (1) D (2) F (3) G (4)							
3d3 2	(2De)	3/2	4d	3	−2.06726E+00	3.28	1 F e
3d3 2	(2De)	3/2	4d	1	−1.94012E+00	3.37	1 P e
3d3 2	(2De)	5/2	4d	2	−1.92280E+00	3.38	1 D e
3d3 2	(2De)	3/2	4d	4	−1.88850E+00	3.46	1 G e
3d3 2	(2De)	5/2	4d	0	−1.84426E+00	3.45	1 S e
$Ncal = 5$: set complete $Nlv = 13, 3$, e:							
S (1) P (2 1 0) D (3 2 1) F (4 3 2) G (5 4 3)							
3d3 2	(2De)	5/2	5d	1	−1.05446E+00	4.36	3 SPD e
3d3 2	(2De)	5/2	5d	5	−1.04247E+00	4.38	3 G e
3d3 2	(2De)	3/2	5d	3	−1.04179E+00	4.38	3 DFG e
3d3 2	(2De)	3/2	5d	1	−1.03332E+00	4.40	3 SPD e
3d3 2	(2De)	5/2	5d	4	−1.03014E+00	4.40	3 FG e
3d3 2	(2De)	5/2	5d	2	−1.02889E+00	4.40	3 PDF e
3d3 2	(2De)	3/2	5d	0	−1.02130E+00	4.42	3 P e
3d3 2	(2De)	5/2	5d	1	−1.01682E+00	4.43	3 SPD e
3d3 2	(2De)	5/2	5d	3	−1.01420E+00	4.43	3 DFG e
3d3 2	(2De)	3/2	5d	2	−1.00936E+00	4.44	3 PDF e
3d3 2	(2De)	3/2	5d	2	−9.92578E-01	4.47	3 PDF e
3d3 2	(2De)	5/2	5d	3	−9.81500E-01	4.49	3 DFG e
$Ncal = 12$, $Nlv = 13$: set incomplete, level missing: 4							
Odd Parity, Equivalent-electron & unidentifiable levels (see discussion)							
3p53d5				1	−1.23559E+00		
3p53d5				2	−1.22406E+00		
3p53d5				6	−1.21757E+00		
3p53d5				5	−1.21176E+00		
3p53d5				4	−1.20632E+00		
3p53d5				3	−1.20599E+00		
3p53d5				3	−1.20156E+00		
3p53d5				2	−1.19775E+00		
3p53d5				4	−1.15378E+00		
3p53d5				3	−1.13582E+00		
3p53d5				2	−1.13085E+00		
3p53d5				5	−1.12662E+00		
3p53d5				2	−1.12076E+00		
3p53d5				4	−1.11088E+00		
3p53d5				0	−1.10428E+00		
3p53d5				2	−1.09132E+00		
3p53d5				7	−1.06928E+00		
3p53d5				6	−1.05100E+00		
3p53d5				1	−1.04259E+00		
3p53d5				3	−1.02720E+00		
3p53d5				4	−9.99298E-01		
3p53d5				1	−9.99223E-01		
3p53d5				3	−9.98823E-01		
3p53d5				5	−9.92970E-01		

is not carried out in the BPRM calculations of bound states, which are entirely ab initio, with the associated advantage of consistent uncertainties for most transitions considered.

To obtain an estimate of the accuracy of the wavefunctions employed in the length and the velocity formulations, we plot, for example, the gf-values for transitions $(J = 1)^{e} - (J = 2)^{o}$ and $(J = 3)^{e} - (J = 4)^{o}$ in Fig. 1. The top panel contains over 13,300 transitions between the pair of symmetries $(J = 1)^{e} - (J = 2)^{o}$, and the bottom panel contains over 20,200 transitions between the pair $(J = 3)^{e} - (J = 4)^{o}$. The plots show practically no dispersion for the strongest transitions with $gf \approx 5 - 10$, and some dispersion around 10–20% for others with $gf < 3$. Up to $gf < 0.1$ the dispersion in length and velocity remains around the 10–20% level for most of the transitions, although the number of outlying transitions increases with decreasing gf. Given the large number of points in the figures, the relatively low dispersion of gf_{L} and gf_{V} indicates that the f-values (gf divided by the statistical weight factor, $2J + 1$) for most of the transitions with $gf \sim 1$ should be within 20% uncertainty. The f_{L}'s are usually more accurate than f_{V}'s since the asymptotic region wavefunctions are more accurately represented in the close coupling calculations using the R-matrix method.

In general the intercombination transitions are weaker than the dipole allowed ones; the f-values can be orders of magnitude lower. The BP Hamiltonian in the present work (Eq. 2) does not include the two-body spin-spin and

Table V. *Transition probabilties of Fe V among observed fine structure levels. Full version available at: http://www.physica.org/digidata/v061p06a00675/tables/tableV.pdf.*

C_i	C_f	$S_iL_i\pi_i$	$S_fL_f\pi_f$	g_i	g_f	E_i (Ry)	E_f (Ry)	f	A_{fi} (s^{-1})
$3d^4$	– $3d^3(4F)4p$	$^5D^e$	$^5F^o$	1	3	5.5132	3.1644	2.154E-01	3.18E+09
$3d^4$	– $3d^3(4F)4p$	$^5D^e$	$^5F^o$	3	3	5.5119	3.1644	3.790E-04	1.68E+07
$3d^4$	– $3d^3(4F)4p$	$^5D^e$	$^5F^o$	3	5	5.5119	3.1496	1.358E-03	3.65E+07
$3d^4$	– $3d^3(4F)4p$	$^5D^e$	$^5F^o$	5	3	5.5094	3.1644	4.617E-02	3.40E+09
$3d^4$	– $3d^3(4F)4p$	$^5D^e$	$^5F^o$	5	5	5.5094	3.1496	5.967E-02	2.67E+09
$3d^4$	– $3d^3(4F)4p$	$^5D^e$	$^5F^o$	5	7	5.5094	3.1443	1.462E-02	4.69E+08
$3d^4$	– $3d^3(4F)4p$	$^5D^e$	$^5F^o$	7	5	5.5058	3.1496	6.895E-03	4.30E+08
$3d^4$	– $3d^3(4F)4p$	$^5D^e$	$^5F^o$	7	7	5.5058	3.1443	5.889E-02	2.64E+09
$3d^4$	– $3d^3(4F)4p$	$^5D^e$	$^5F^o$	9	7	5.5015	3.1443	1.966E-03	1.13E+08
$3d^4$	– $3d^3(4F)4p$	$^5D^e$	$^5F^o$	7	9	5.5058	3.1391	3.262E-02	1.14E+09
$3d^4$	– $3d^3(4F)4p$	$^5D^e$	$^5F^o$	9	9	5.5015	3.1391	5.139E-02	2.30E+09
$3d^4$	– $3d^3(4F)4p$	$^5D^e$	$^5F^o$	9	11	5.5015	3.1343	7.548E-02	2.78E+09
LS				25	35	5.5055	3.1451	1.068E-01	3.42E+09
$3d^4$	– $3d^3(4F)4p$	$^5D^e$	$^5D^o$	1	3	5.5132	3.1540	5.515E-03	8.22E+07
$3d^4$	– $3d^3(4F)4p$	$^5D^e$	$^5D^o$	3	1	5.5119	3.1565	6.255E-02	8.36E+09
$3d^4$	– $3d^3(4F)4p$	$^5D^e$	$^5D^o$	3	3	5.5119	3.1540	3.888E-02	1.74E+09
$3d^4$	– $3d^3(4F)4p$	$^5D^e$	$^5D^o$	3	5	5.5119	3.1609	1.360E-01	3.62E+09
$3d^4$	– $3d^3(4F)4p$	$^5D^e$	$^5D^o$	5	3	5.5094	3.1540	1.704E-02	1.27E+09
$3d^4$	– $3d^3(4F)4p$	$^5D^e$	$^5D^o$	5	5	5.5094	3.1609	1.372E-02	6.08E+08
$3d^4$	– $3d^3(4F)4p$	$^5D^e$	$^5D^o$	5	7	5.5094	3.1559	1.087E-01	3.45E+09
$3d^4$	– $3d^3(4F)4p$	$^5D^e$	$^5D^o$	7	5	5.5058	3.1609	4.155E-02	2.57E+09
$3d^4$	– $3d^3(4F)4p$	$^5D^e$	$^5D^o$	7	7	5.5058	3.1559	4.936E-02	2.19E+09
$3d^4$	– $3d^3(4F)4p$	$^5D^e$	$^5D^o$	9	7	5.5015	3.1559	2.644E-02	1.50E+09
$3d^4$	– $3d^3(4F)4p$	$^5D^e$	$^5D^o$	7	9	5.5058	3.1498	7.311E-02	2.54E+09
$3d^4$	– $3d^3(4F)4p$	$^5D^e$	$^5D^o$	9	9	5.5015	3.1498	1.168E-01	5.19E+09
LS				25	25	5.5064	3.1551	1.541E-01	6.84E+09
$3d^4$	– $3d^3(4F)4p$	$^5D^e$	$^3D^o$	1	3	5.5132	3.1439	5.744E-02	8.63E+08
$3d^4$	– $3d^3(4F)4p$	$^5D^e$	$^3D^o$	3	3	5.5119	3.1439	6.807E-03	3.07E+08
$3d^4$	– $3d^3(4F)4p$	$^5D^e$	$^3D^o$	3	5	5.5119	3.1401	3.147E-02	8.53E+08
$3d^4$	– $3d^3(4F)4p$	$^5D^e$	$^3D^o$	5	3	5.5094	3.1439	4.980E-03	3.73E+08
$3d^4$	– $3d^3(4F)4p$	$^5D^e$	$^3D^o$	5	5	5.5094	3.1401	2.987E-07	1.35E+04
$3d^4$	– $3d^3(4F)4p$	$^5D^e$	$^3D^o$	5	7	5.5094	3.1331	1.149E-02	3.72E+08
$3d^4$	– $3d^3(4F)4p$	$^5D^e$	$^3D^o$	7	5	5.5058	3.1401	6.830E-03	4.30E+08
$3d^4$	– $3d^3(4F)4p$	$^5D^e$	$^3D^o$	7	7	5.5058	3.1331	4.107E-03	1.86E+08
$3d^4$	– $3d^3(4F)4p$	$^5D^e$	$^3D^o$	9	7	5.5015	3.1331	3.671E-03	2.13E+08
$3d^4$	– $3d^3(4P)4p$	$^5D^e$	$^5P^o$	1	3	5.5132	3.0195	8.420E-02	1.40E+09
$3d^4$	– $3d^3(4P)4p$	$^5D^e$	$^5P^o$	3	3	5.5119	3.0195	6.281E-02	3.13E+09
$3d^4$	– $3d^3(4P)4p$	$^5D^e$	$^5P^o$	3	5	5.5119	3.0151	2.114E-02	6.35E+08
$3d^4$	– $3d^3(4P)4p$	$^5D^e$	$^5P^o$	5	3	5.5094	3.0195	2.926E-02	2.43E+09
$3d^4$	– $3d^3(4P)4p$	$^5D^e$	$^5P^o$	5	5	5.5094	3.0151	4.831E-02	2.41E+09
$3d^4$	– $3d^3(4P)4p$	$^5D^e$	$^5P^o$	5	7	5.5094	3.0078	6.221E-03	2.23E+08
$3d^4$	– $3d^3(4P)4p$	$^5D^e$	$^5P^o$	7	5	5.5058	3.0151	5.555E-02	3.88E+09
$3d^4$	– $3d^3(4P)4p$	$^5D^e$	$^5P^o$	7	7	5.5058	3.0078	3.105E-02	1.56E+09
$3d^4$	– $3d^3(4P)4p$	$^5D^e$	$^5P^o$	9	7	5.5015	3.0078	8.781E-02	5.64E+09
LS				25	15	5.5071	3.0126	8.610E-02	7.17E+09
$3d^4$	– $3d^3(4P)4p$	$^5D^e$	$^5D^o$	1	3	5.5132	3.0058	4.401E-03	7.41E+07
$3d^4$	– $3d^3(4P)4p$	$^5D^e$	$^5D^o$	3	1	5.5119	3.0094	4.902E-04	7.40E+07
$3d^4$	– $3d^3(4P)4p$	$^5D^e$	$^5D^o$	3	3	5.5119	3.0058	7.201E-04	3.63E+07
$3d^4$	– $3d^3(4P)4p$	$^5D^e$	$^5D^o$	3	5	5.5119	2.9912	2.402E-03	7.35E+07
$3d^4$	– $3d^3(4P)4p$	$^5D^e$	$^5D^o$	5	3	5.5094	3.0058	1.502E-03	1.26E+08
$3d^4$	– $3d^3(4P)4p$	$^5D^e$	$^5D^o$	5	5	5.5094	2.9912	2.248E-03	1.14E+08
$3d^4$	– $3d^3(4P)4p$	$^5D^e$	$^5D^o$	5	7	5.5094	2.9883	1.474E-03	5.38E+07
$3d^4$	– $3d^3(4P)4p$	$^5D^e$	$^5D^o$	7	5	5.5058	2.9912	2.675E-03	1.90E+08
$3d^4$	– $3d^3(4P)4p$	$^5D^e$	$^5D^o$	7	7	5.5058	2.9883	1.048E-03	5.33E+07
$3d^4$	– $3d^3(4P)4p$	$^5D^e$	$^5D^o$	9	7	5.5015	2.9883	2.846E-06	1.86E+05
$3d^4$	– $3d^3(4P)4p$	$^5D^e$	$^5D^o$	7	9	5.5058	2.9792	1.408E-03	5.61E+07
$3d^4$	– $3d^3(4P)4p$	$^5D^e$	$^5D^o$	9	9	5.5015	2.9792	4.558E-03	2.33E+08
LS				25	25	5.5064	2.9892	4.731E-03	2.41E+08

Table V. *Continued.*

C_i	C_f	$S_iL_i\pi_i$	$S_fL_f\pi_f$	g_i	g_f	E_i (*Ry*)	E_f (*Ry*)	f	A_{fi} (s^{-1})
$3d^4$	– $3d^3(4P)4p$	$^5D^e$	$^3P^o$	1	3	5.5132	2.9911	8.365E-05	1.42E+06
$3d^4$	– $3d^3(4P)4p$	$^5D^e$	$^3P^o$	3	1	5.5119	2.9941	1.179E-03	1.80E+08
$3d^4$	– $3d^3(4P)4p$	$^5D^e$	$^3P^o$	3	3	5.5119	2.9911	4.467E-04	2.28E+07
$3d^4$	– $3d^3(4P)4p$	$^5D^e$	$^3P^o$	3	5	5.5119	3.0038	4.331E-04	1.31E+07
$3d^4$	– $3d^3(4P)4p$	$^5D^e$	$^3P^o$	5	3	5.5094	2.9911	1.298E-05	1.10E+06
$3d^4$	– $3d^3(4P)4p$	$^5D^e$	$^3P^o$	5	5	5.5094	3.0038	9.745E-05	4.91E+06
$3d^4$	– $3d^3(4P)4p$	$^5D^e$	$^3P^o$	7	5	5.5058	3.0038	1.164E-04	8.19E+06
$3d^4$	– $3d^3(2P)4p$	$^5D^e$	$^3P^o$	1	3	5.5132	2.9439	1.035E-03	1.83E+07
$3d^4$	– $3d^3(2P)4p$	$^5D^e$	$^3P^o$	3	1	5.5119	2.9413	2.456E-08	3.91E+03
$3d^4$	– $3d^3(2P)4p$	$^5D^e$	$^3P^o$	3	3	5.5119	2.9439	4.505E-04	2.39E+07
$3d^4$	– $3d^3(2P)4p$	$^5D^e$	$^3P^o$	3	5	5.5119	2.8668	2.963E-05	9.99E+05
$3d^4$	– $3d^3(2P)4p$	$^5D^e$	$^3P^o$	5	3	5.5094	2.9439	6.224E-04	5.48E+07
$3d^4$	– $3d^3(2P)4p$	$^5D^e$	$^3P^o$	5	5	5.5094	2.8668	2.903E-05	1.63E+06
$3d^4$	– $3d^3(2P)4p$	$^5D^e$	$^3P^o$	7	5	5.5058	2.8668	3.718E-05	2.91E+06
$3d^4$	– $3d^3(2D2)4p$	$^5D^e$	$^1P^o$	1	3	5.5132	2.9073	1.306E-08	2.38E+02
$3d^4$	– $3d^3(2D2)4p$	$^5D^e$	$^1P^o$	3	3	5.5119	2.9073	1.655E-06	9.02E+04
$3d^4$	– $3d^3(2D2)4p$	$^5D^e$	$^1P^o$	5	3	5.5094	2.9073	9.168E-06	8.31E+05
$3d^4$	– $3d^3(2D2)4p$	$^5D^e$	$^3D^o$	1	3	5.5132	2.8826	2.062E-06	3.82E+04
$3d^4$	– $3d^3(2D2)4p$	$^5D^e$	$^3D^o$	3	3	5.5119	2.8826	5.025E-06	2.79E+05
$3d^4$	– $3d^3(2D2)4p$	$^5D^e$	$^3D^o$	3	5	5.5119	2.8761	1.691E-05	5.66E+05
$3d^4$	– $3d^3(2D2)4p$	$^5D^e$	$^3D^o$	5	3	5.5094	2.8826	2.087E-07	1.93E+04
$3d^4$	– $3d^3(2D2)4p$	$^5D^e$	$^3D^o$	5	5	5.5094	2.8761	1.929E-05	1.07E+06
$3d^4$	– $3d^3(2D2)4p$	$^5D^e$	$^3D^o$	5	7	5.5094	2.8713	3.481E-05	1.39E+06
$3d^4$	– $3d^3(2D2)4p$	$^5D^e$	$^3D^o$	7	5	5.5058	2.8761	1.622E-06	1.26E+05
$3d^4$	– $3d^3(2D2)4p$	$^5D^e$	$^3D^o$	7	7	5.5058	2.8713	2.264E-02	1.26E+09
$3d^4$	– $3d^3(2D2)4p$	$^5D^e$	$^3D^o$	9	7	5.5015	2.8713	1.661E-05	1.19E+06
$3d^4$	– $3d^3(2D2)4p$	$^5D^e$	$^3D^o$	7	9	5.5058	2.8761	6.490E-10	2.80E+01
$3d^4$	– $3d^3(2D2)4p$	$^5D^e$	$^3D^o$	9	9	5.5015	2.8761	4.627E-08	2.56E+03
$3d^4$	– $3d^3(2P)4p$	$^5D^e$	$^3D^o$	1	3	5.5132	2.9274	1.222E-03	2.19E+07
$3d^4$	– $3d^3(2P)4p$	$^5D^e$	$^3D^o$	3	3	5.5119	2.9274	8.954E-04	4.80E+07
$3d^4$	– $3d^3(2P)4p$	$^5D^e$	$^3D^o$	3	5	5.5119	2.9169	2.958E-06	9.60E+04
$3d^4$	– $3d^3(2P)4p$	$^5D^e$	$^3D^o$	5	3	5.5094	2.9274	3.739E-04	3.34E+07
$3d^4$	– $3d^3(2P)4p$	$^5D^e$	$^3D^o$	5	5	5.5094	2.9169	9.819E-06	5.30E+05
$3d^4$	– $3d^3(2P)4p$	$^5D^e$	$^3D^o$	5	7	5.5094	2.9117	3.148E-06	1.22E+05
$3d^4$	– $3d^3(2P)4p$	$^5D^e$	$^3D^o$	7	5	5.5058	2.9169	9.881E-06	7.45E+05
$3d^4$	– $3d^3(2P)4p$	$^5D^e$	$^3D^o$	7	7	5.5058	2.9117	1.265E-03	6.84E+07
$3d^4$	– $3d^3(2P)4p$	$^5D^e$	$^3D^o$	9	7	5.5015	2.9117	1.136E-05	7.87E+05
$3d^4$	– $3d^3(2P)4p$	$^5D^e$	$^3S^o$	1	3	5.5132	2.9052	4.138E-06	7.54E+04
$3d^4$	– $3d^3(2P)4p$	$^5D^e$	$^3S^o$	3	3	5.5119	2.9052	1.659E-08	9.05E+02
$3d^4$	– $3d^3(2P)4p$	$^5D^e$	$^3S^o$	5	3	5.5094	2.9052	6.255E-07	5.68E+04
$3d^4$	– $3d^3(4P)4p$	$^5D^e$	$^3D^o$	1	3	5.5132	2.8991	4.318E-06	7.90E+04
$3d^4$	– $3d^3(4P)4p$	$^5D^e$	$^3D^o$	3	3	5.5119	2.8991	1.262E-06	6.92E+04
$3d^4$	– $3d^3(4P)4p$	$^5D^e$	$^3D^o$	3	5	5.5119	2.8991	9.987E-07	3.29E+04
$3d^4$	– $3d^3(4P)4p$	$^5D^e$	$^3D^o$	5	3	5.5094	2.8991	2.563E-06	2.34E+05
$3d^4$	– $3d^3(4P)4p$	$^5D^e$	$^3D^o$	5	5	5.5094	2.8991	3.397E-08	1.86E+03
$3d^4$	– $3d^3(4P)4p$	$^5D^e$	$^3D^o$	5	7	5.5094	2.9030	6.662E-05	2.60E+06
$3d^4$	– $3d^3(4P)4p$	$^5D^e$	$^3D^o$	7	5	5.5058	2.8991	1.275E-06	9.74E+04
$3d^4$	– $3d^3(4P)4p$	$^5D^e$	$^3D^o$	7	7	5.5058	2.9030	1.589E-02	8.65E+08
$3d^4$	– $3d^3(4P)4p$	$^5D^e$	$^3D^o$	9	7	5.5015	2.9030	7.636E-05	5.32E+06
$3d^4$	– $3d^3(2D2)4p$	$^5D^e$	$^3P^o$	1	3	5.5132	2.8652	3.020E-05	5.67E+05
$3d^4$	– $3d^3(2D2)4p$	$^5D^e$	$^3P^o$	3	1	5.5119	2.8623	1.555E-05	2.63E+06
$3d^4$	– $3d^3(2D2)4p$	$^5D^e$	$^3P^o$	3	3	5.5119	2.8652	1.906E-05	1.07E+06
$3d^4$	– $3d^3(2D2)4p$	$^5D^e$	$^3P^o$	5	3	5.5094	2.8652	6.600E-06	6.18E+05
$3d^4$	– $3d^3(2P)4p$	$^5D^e$	$^1P^o$	1	3	5.5132	2.8161	2.397E-06	4.67E+04
$3d^4$	– $3d^3(2P)4p$	$^5D^e$	$^1P^o$	3	3	5.5119	2.8161	2.381E-06	1.39E+05
$3d^4$	– $3d^3(2P)4p$	$^5D^e$	$^1P^o$	5	3	5.5094	2.8161	3.000E-06	2.91E+05
$3d^4$	– $3d^3(4P)4p$	$^5D^e$	$^3S^o$	1	3	5.5132	2.8282	6.009E-05	1.16E+06
$3d^4$	– $3d^3(4P)4p$	$^5D^e$	$^3S^o$	3	3	5.5119	2.8282	4.589E-05	2.65E+06
$3d^4$	– $3d^3(4P)4p$	$^5D^e$	$^3S^o$	5	3	5.5094	2.8282	2.678E-05	2.58E+06

Table V. *Continued.*

C_i	C_f	$S_iL_i\pi_i$	$S_fL_f\pi_f$	g_i	g_f	E_i (*Ry*)	E_f (*Ry*)	f	A_{fi} (s^{-1})
$3d^4$	– $3d^3$(2F)4p	$^5D^e$	$^3D^o$	1	3	5.5132	2.7003	4.619E-06	9.78E+04
$3d^4$	– $3d^3$(2F)4p	$^5D^e$	$^3D^o$	3	3	5.5119	2.7003	6.420E-07	4.08E+04
$3d^4$	– $3d^3$(2F)4p	$^5D^e$	$^3D^o$	3	5	5.5119	2.7050	3.933E-09	1.49E+02
$3d^4$	– $3d^3$(2F)4p	$^5D^e$	$^3D^o$	5	3	5.5094	2.7003	4.515E-08	4.77E+03
$3d^4$	– $3d^3$(2F)4p	$^5D^e$	$^3D^o$	5	5	5.5094	2.7050	6.185E-06	3.91E+05
$3d^4$	– $3d^3$(2F)4p	$^5D^e$	$^3D^o$	5	7	5.5094	2.7129	7.193E-07	3.23E+04
$3d^4$	– $3d^3$(2F)4p	$^5D^e$	$^3D^o$	7	5	5.5058	2.7050	1.201E-07	1.06E+04
$3d^4$	– $3d^3$(2F)4p	$^5D^e$	$^3D^o$	7	7	5.5058	2.7129	6.082E-05	3.81E+06
$3d^4$	– $3d^3$(2F)4p	$^5D^e$	$^3D^o$	9	7	5.5015	2.7129	6.629E-06	5.32E+05

Table VI. *Comparison of present (P) f-values with the earlier ones. Full version available at: http://www.physica.org/digidata/v061p06a00675/tables/tableVI.pdf.*

C_i	C_j	$S_iL_i\pi_i$	$S_jL_j\pi_j$	$2J_i+1$	I_i	$2J_j+1$	I_j	$f_{ij}(P)$	f_{ij} (others)
3d4	–3d3(4F)4p	5D0	5F1	1	1	3	1	0.2154	0.163[a]
3d4	–3d3(4F)4p	5D0	5F1	3	1	3	1	3.790E-04	
3d4	–3d3(4F)4p	5D0	5F1	3	1	5	3	0.00136	
3d4	–3d3(4F)4p	5D0	5F1	5	1	3	1	0.04617	0.0126[a]
3d4	–3d3(4F)4p	5D0	5F1	5	1	5	3	0.05967	0.0596[a]
3d4	–3d3(4F)4p	5D0	5F1	5	1	7	3	0.01462	0.0138[a]
3d4	–3d3(4F)4p	5D0	5F1	7	1	5	3	0.006895	0.0274[a]
3d4	–3d3(4F)4p	5D0	5F1	7	1	7	3	0.05889	0.0544[a]
3d4	–3d3(4F)4p	5D0	5F1	9	1	7	3	0.001966	0.00756[a]
3d4	–3d3(4F)4p	5D0	5F1	7	1	9	3	0.03262	0.0414[a]
3d4	–3d3(4F)4p	5D0	5F1	9	1	9	3	0.05139	0.03[a]
3d4	–3d3(4F)4p	5D0	5F1	9	1	11	2	0.07548	0.0686[a]
3d4	–3d3(4F)4p	5D0	5F1	25		35		0.107	0.0804[b], 0.0915[c]
3d4	–3d3(4F)4p	5D0	5D1	1	1	3	2	0.00551	0.041[a]
3d4	–3d3(4F)4p	5D0	5D1	3	1	1	1	0.06255	0.0607[a]
3d4	–3d3(4F)4p	5D0	5D1	3	1	3	2	0.03888	0.0343[a]
3d4	–3d3(4F)4p	5D0	5D1	3	1	5	2	0.1360	0.1257[a]
3d4	–3d3(4F)4p	5D0	5D1	5	1	3	2	0.01704	0.0532[a]
3d4	–3d3(4F)4p	5D0	5D1	5	1	5	2	0.01372	0.0092[a]
3d4	–3d3(4F)4p	5D0	5D1	5	1	7	2	0.1087	0.1006[a]
3d4	–3d3(4F)4p	5D0	5D1	7	1	5	2	0.04155	0.0247[a]
3d4	–3d3(4F)4p	5D0	5D1	7	1	7	2	0.04936	0.0517[a]
3d4	–3d3(4F)4p	5D0	5D1	9	1	7	2	0.02644	0.0222[a]
3d4	–3d3(4F)4p	5D0	5D1	7	1	9	2	0.07311	0.0588[a]
3d4	–3d3(4F)4p	5D0	5D1	9	1	9	2	0.1168	0.130[a]
3d4	–3d3(4F)4p	5D0	5D1	25		25		0.1541	0.1708[b],0.192[c]
3d4	–3d3(4P)4p	5D0	5P1	1	1	3	4	0.08420	0.076[a]
3d4	–3d3(4P)4p	5D0	5P1	3	1	3	4	0.06281	0.057[a]
3d4	–3d3(4P)4p	5D0	5P1	3	1	5	6	0.02114	0.019[a]
3d4	–3d3(4P)4p	5D0	5P1	5	1	3	4	0.02926	0.0266[a]
3d4	–3d3(4P)4p	5D0	5P1	5	1	5	6	0.04831	0.0442[a]
3d4	–3d3(4P)4p	5D0	5P1	5	1	7	7	0.00622	0.0054[a]
3d4	–3d3(4P)4p	5D0	5P1	7	1	5	6	0.05555	0.0499[a]
3d4	–3d3(4P)4p	5D0	5P1	7	1	7	7	0.03105	0.0264[a]
3d4	–3d3(4P)4p	5D0	5P1	9	1	7	7	0.08782	0.0758[a]
3d4	–3d3(4P)4p	5D0	5P1	25		15		0.0861	0.076[b],0.0893[c]

[a]Fawcett (1989), [b]Butler (TOPbase), [c]Bautista (1996).

spin-other-orbit terms of Breit interaction [22]. A discussion of these terms is given by Mendoza *et al.* in a recent IP paper [27]. Their study on the intercombination transitions in C-like ions shows that the effect of the two-body Breit terms, relative to the one-body operators, decreases with Z such that for $Z = 26$ the computed A-values with and without the two-body Breit terms differ by less than 0.5 %. However, the differences towards the neutral end of the C-sequence is up to about 20%. It may therefore be expected that for Fe V the weaker intercombination f-values may also be systematically affected to a similar extent (the uncertainties in the dipole allowed f-values should be much less). Further studies of the Breit interaction in complex atoms are needed to ascertain this effect more precisely.

Several aspects of the present work are targets for future studies, such as atomic structure calculations to study the

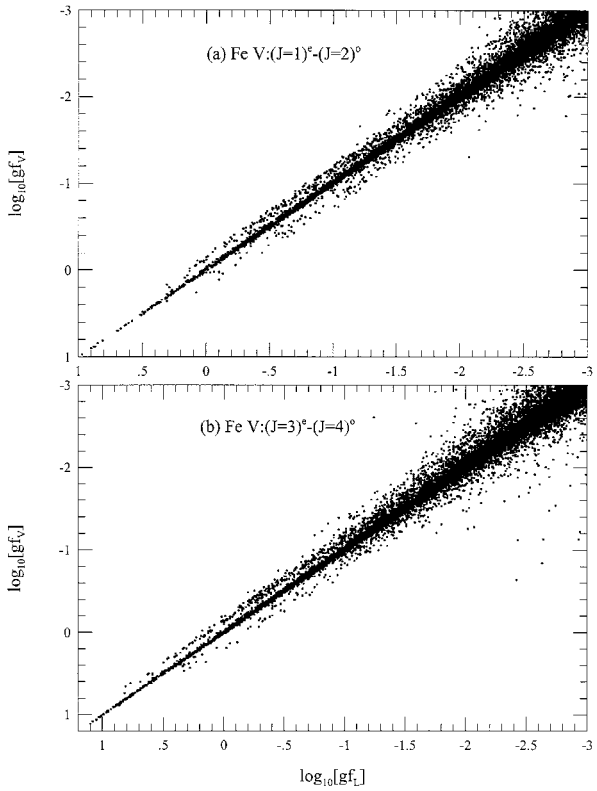

Fig. 1. Comprarison of gf_L vs gf_V for bound-bound fine structure level transitions in Fe V obtained in BPRM approximation.

effect of configuration interaction and relativistic effects on different types of transitions, and a detailed quantum defect analysis along interacting Rydberg series of levels in intermediate coupling. These studies should provide information on the accuracy of particular type of transitions and groups of levels, as well as address general problems in the analysis of complex spectra.

5. Conclusion

The present work is the first study of large-scale transition probabilities computed using the accurate BPRM method for a highly complex ion. Some of the results obtained herein are expected to form the basis for future computational spectroscopy of heretofore intractable complex atomic systems using efficient collision theory methods. The computational procedures developed for such undertakings are described, and illustrative results are presented from the *ab initio* Breit–Pauli R-matrix calculations for Fe V. Detailed analysis for the identification of over 3,800 fine structure levels of Fe V is carried out using a combination of methods that include quantum defect theory. Further work on the analysis of relativistic quantum defects in intermediate coupling is planned.

Following the completion of all computations and identifications, the dataset of approximately 1.5 million oscillator strengths will be described in another publication with a view towards astrophysical and laboratory applications. In order to complete the dataset for practical applications calculations are also in progress for the forbidden electric quadrupole and magnetic dipole transition probabilties using the atomic structure program SUPERSTRUCTURE.

The newly acquired theoretical capability to obtain an essentially complete description of radiative transitions for an atomic system should enable several new advances such as: (a) the synthesis of highly detailed monochromatic opacity spectra [2], (b) the simulation of ''quasi-continuum'' line spectra from iron ions [28], (c) high resolution spectral diagnostics of iron in laboratory fusion and astrophysical sources, and (d) the analysis of experimentally measured spectra of complex iron ions.

Acknowledgements

This work was supported partially by the U.S. National Science Foundation (AST-9870089) and the NASA (NAG5-7903). The computational work was carried out at the Ohio Supercomputer Center in Columbus Ohio.

References

1. Fuhr, J. R., Martin, G. A. and Wiese, W. L., J. Phys. Chem. Ref. Data **17**, Suppl No. 4 (1988)
2. Seaton, M. J., Yu, Y., Mihalas, D. and Pradhan, A. K., MNRAS **266**, 805 (1994).
3. Rogers, F. J. and Iglesias C. A., Science **263**, 50 (1994).
4. Chayer, P., Fontaine, G. and Wesemael, F., Astrophys. J. **99**, 189 (1995).
5. Becker, S. R. and Butler, K., Astron. Astrophys. **265**, 647 (1992)
6. Vennes, S., ''Astrophysics in the Extreme Ultraviolet,'' (eds. Stuart Bowyer and Roger F. Malina), (Kluwer, 1996) p. 185; Pradhan, A. K., Ibid., p. 569.
7. Seaton, M. J., J. Phys. B **20**, 6363 (1987).
8. Hummer, D. G. *et al.*, Astron. Astrophys. **279**, 298 (1993).
9. Burke, P. G., Hibbert, A. and Robb, J. Physics B **4**, 153 (1971).
10. Berrington, K. A. *et al.*, J. Phys. B **20** 6379 (1987).
11. Nahar, S. N. and Pradhan, A. K., Astron. Astrophys. Suppl. Ser. **135**, 347 (1999).
12. Zhang, H. L., Phys. Rev. A **57**, 2640 (1998).
13. Zhang, H. L., Nahar S. N. and Pradhan, A. K., J. Phys. B **32**, 1459 (1999).
14. Johnson, W. R., Liu Z. W. and Sapirstein, J., At. Data Nucl. Data **64**, 279 (1996).
15. Yan, Z-C, Tambasco, M. and Drake, G. W. F., Phys. Rev. A **57**, 1652 (1998).
16. Burke, P. G. and Seaton M. J., J. Physics B **17**, L683 (1984).
17. Seaton, M. J., J. Phys. B **18**, 2111 (1985).
18. Scott, N. S., Taylor, K. T., Comput. Phys. Commun. **25**, 347 (1982).
19. Berrington, K. A., Eissner, W., Norrington, P. H., Comput. Phys. Commun. **92**, 290 (1995).
20. Burke, P. G. and Berrington, K. A., ''Atomic and Molecular Processes, an R-matrix Approach,'' Institute of Physics Publishing, Bristol (1993)
21. Chen, G. X. and Pradhan, A. K., J. Phys. B **32**, 1809 (1999a); Astron. Astrophys. Suppl. **136**, 395 (1999b).
22. Eissner, W., Jones, M. and Nussbaumer, H., Comput. Phys. Commun **8**, 270 (1974); Eissner, W., J. Phys. IV (Paris) C1, 3 (1991), Eissner, W. (in preparation, 2000).
23. Sugar, J. and Corliss, C., J. Phys. Chem. Ref. Data 14, Suppl. **2** (1985).
24. Butler, K. (unpublished); data are available through the OP database, TOPbase (Cunto, W., Mendoza, C., Ochsenbein, F., Zeippen, C., Astron. Astrophys **275**, L5 (1993)).
25. Bautista, M. A., Astron. Astrophys. Suppl. Ser. **119**, 105 (1996).
26. Fawcett, B. C., At. Data Nucl. Data Tables **41**, 181 (1989).
27. Mendoza, C., Zeippen, C. J. and Storey, P. J., Astron. Astrophys. Suppl. Ser. **135**, 159 (1999).
28. Beirsdorfer, P. *et al.*, Astrophys. J. **519**, L185 (1999).

